BB

LBL-36732
UC-413

Lawrence Berkeley Laboratory
UNIVERSITY OF CALIFORNIA

Presented at the XVIIIth Nuclear Physics Symposium at Oaxtepec, Oaxtepec, Mexico, January 4–7, 1995, and to be published in the Proceedings

Experimental Evidence for the Reducibility of Multifragment Emission Probabilities

G.J. Wozniak, K. Tso, L. Phair, N. Colonna, W. Skulski, K. Jing, L.G. Moretto, D.R. Bowman, N. Carlin, C.K. Gelbke, W.G. Gong, W.C. Hsi, Y.D. Kim, M.A. Lisa, W.G. Lynch, M. Chartier, G.F. Peaslee, C. Schwarz, R.T. de Souza, M.B. Tsang, and F. Zhu

January 1995

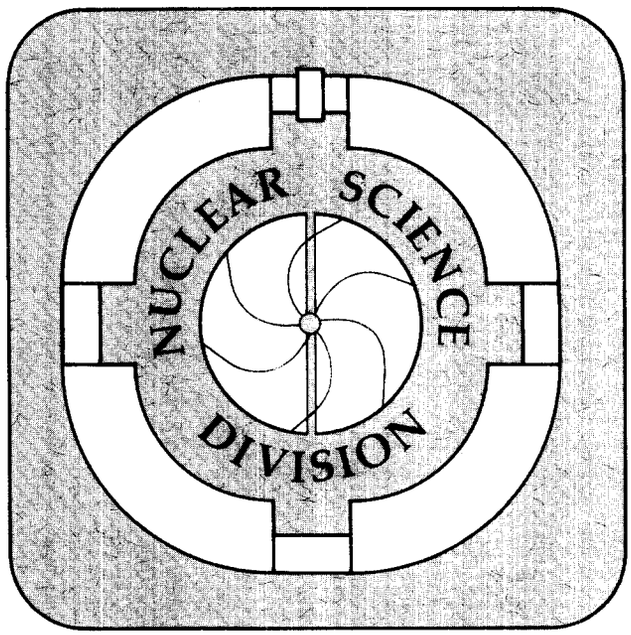

Prepared for the U.S. Department of Energy under Contract Number DE-AC03-76SF00098

LBL - 36732
UC 413

Experimental Evidence for the Reducibility of Multifragment Emission Probabilities

G.J. Wozniak, K. Tso, L. Phair, N. Colonna, W. Skulski, K. Jing, and L.G. Moretto
Nuclear Science Division, Lawrence Berkeley Laboratory
University of California, Berkeley, California 94720, USA

D.R. Bowman, N. Carlin, C.K. Gelbke, W.G. Gong, W.C. Hsi, Y.D. Kim, M.A. Lisa, W.G. Lynch, M. Chartier, G.F. Peaslee, C. Schwarz, R.T. de Souza, M.B. Tsang, and F. Zhu
National Superconducting Cyclotron Laboratory, Michigan State University, E. Lansing, MI 48824

January 1995

This work was supported by the Director, Office of Energy Research Division of Nuclear Physics of the Office of High Energy and Nuclear Physics of the U.S. Department of Energy under Contract DE-AC03-76SF00098

Experimental Evidence for the Reducibility of Multifragment Emission Probabilities

G. J. Wozniak, K. Tso, L. Phair, N. Colonna[a], W. Skulski[b], K. Jing, and L.G. Moretto
Nuclear Science Division, Lawrence Berkeley Laboratory, Berkeley, CA 94720

D. R. Bowman[c], N. Carlin[d], C. K. Gelbke, W. G. Gong[e], W.C. Hsi, Y. D. Kim[f], M. A. Lisa[e], W. G. Lynch, M. Chartier[g], G. F. Peaslee[h], C. Schwarz[i], R. T. de Souza[j], M. B. Tsang, and F. Zhu[k]
National Superconducting Cyclotron Laboratory, Michigan State University, E. Lansing, MI 48824

Abstract: Multifragmentation has been studied for ^{36}Ar-induced reactions on a ^{197}Au target at E/A = 80 and 110 MeV and for ^{129}Xe-induced reactions on several targets (^{nat}Cu, ^{89}Y, ^{165}Ho, ^{197}Au) at E/A = 40, 50 and 60 MeV. The probability of emitting *n* intermediate-mass-fragments is shown to be binomial at each transversal energy and reducible to an elementary binary probability *p*. For each target and at each bombarding energy, this probability *p* shows a thermal nature by giving linear Arrhenius plots. For the ^{129}Xe-induced reactions, a nearly universal linear Arrhenius plot is observed at each bombarding energy, indicating a large degree of target independence.

Introduction

At low excitation energies, complex fragments are emitted with low probability by a compound nucleus mechanism[1, 2]. At increasingly larger energies, the probability of complex fragment emission increases dramatically, until several fragments are observed within a single event [3-6]. The nature of this multifragmentation process is at the center of much current attention. For example, the time-scale of fragment emission and the associated issue of sequentiality versus simultaneity are the objects of intense theoretical[3-9] and experimental [10-18] study.

Recent experimental work[19, 20] has shown that the excitation functions for the production of two, three, four, etc. fragments give a characteristically linear Arrhenius plot[21], suggesting a statistical energy dependence.

A fundamental issue, connected in part to those mentioned above, is that of reducibility: can multifragmentation be reduced to a combination of (nearly) independent emissions of fragments? More to the point, can the probability for the emission of n fragments be reduced to the emission probability of just one fragment?

In what follows, we show evidence that the n-fragment emission probabilities are indeed reducible to an elementary binary emission probability. Furthermore, we shall show that the energy dependence of the extracted elementary probabilities gives a linear Arrhenius plot. Thus, these probabilities are likely to be thermal. While reducibility does not strictly imply time sequentiality, in what follows we point out the time implications associated with a temporal reading of a reducible thermal theory.

Reducibility

The partial decay width Γ associated with a given binary channel can be approximated by:

$$\Gamma = \hbar\omega_o e^{-B/T}, \tag{1}$$

where ω_o is a frequency characteristic of the channel under consideration, B is the barrier associated with the channel, and T is the temperature. For instance, in fission ω_o is the collective frequency of assault on the barrier (~ beta vibration frequency) and B is the fission barrier.

The elementary probability p for a binary decay to occur at any given "try" defined by the channel period $\tau_o = 1/\omega_o$ is:

$$p = \frac{\Gamma}{\hbar\omega_o} = e^{-B/T}. \tag{2}$$

The corresponding time τ is given by:

$$\tau = \tau_o e^{B/T}. \tag{3}$$

In the case of a compound nucleus, the total decay width is the sum of the widths of all channels, and the lifetime is calculated accordingly. For the case of sequential multifragmentation, only the decay width and lifetime for binary fragment formation need be

considered, while the abundant light particle decay can be treated as a background that may progressively modify the temperature and possibly the barrier.

Now, we note that the elementary binary probability p can be directly related to the experimental branching ratios for binary, ternary, quaternary, etc., decay. For simplicity, let us assume that the system has the opportunity to try m times to emit an "inert" fragment with constant probability p. The probability P_n^m of emitting exactly n fragments is given by the binomial distribution:

$$P_n^m = \frac{m!}{n!(m-n)!} p^n (1-p)^{m-n} . \tag{4}$$

The average multiplicity is then

$$\langle n \rangle = mp \tag{5}$$

and the variance

$$\sigma_n^2 = \langle n \rangle (1-p) . \tag{6}$$

It should be pointed out that this is a rather special way to build multifragment probabilities from binary probabilities. It has been chosen "a posteriori" because it happens to work extremely well. Other ways associated with different decay branchings (e.g., each produced fragment can, in turn, decay into two fragments with probability p) yield nonbinomial distributions.

From the experimental values of $\langle n \rangle$ and σ_n^2 one can extract values for p and m, at any excitation energy. Alternatively, one can extract p from the ratio of any pair of excitation functions $P_n^m(T)$:

$$\frac{1}{p} = \frac{\tau}{\tau_o} = \frac{P_n^m}{P_{n+1}^m} \frac{m-n}{n+1} + 1 . \tag{7}$$

Experimental Technique

The experiments were performed at the K1200 Cyclotron of the National Superconducting Laboratory at Michigan State University. ^{36}Ar beams of E/A = 80 and 110 MeV were used to bombard a ^{197}Au target. ^{129}Xe beams of E/A = 40, 50 and 60 MeV were used to bombard

several targets (^{nat}Cu, ^{89}Y, ^{165}Ho, ^{197}Au). Reaction products (Z = 1 - 54) were detected with a multidetector system consisting of the MSU Miniball phoswich array[22] and the LBL forward array[23]. The combined detector system covered a large fraction of the available solid angle (89% of 4π). The Miniball (171 phoswich detectores) was used to identify charged particles with Z = 1 - 20 emitted between 16° and 160° with respect to the beam axis. At forward angles, from 2° to 16°, charged particles with Z = 1 - 54 were detected by the 16 Si-Si-Plastic telescopes of the LBL array. The energies of the fragments detected in the forward array were measured to better than 1% and positions to ±1.5mm. Representative detection thresholds for the Miniball and the LBL array were E/A = 2, 3, 4 MeV for Z = 3, 10, 18 and E/A = 6, 13, 21, 21 MeV for Z = 2, 8, 20, 54, respectively.

^{36}Ar-Induced Reactions

We now proceed to examine the experimental data for signatures of reducibility. References [24,25] report values of $\langle n \rangle$ and σ_n^2 for the reaction ^{36}Ar + ^{197}Au at 80 & 110 MeV/u (available center-of-mass energy of 2.4 and 3.3 GeV, respectively) as a function of the transversal energy E_t. It is defined as $E_t = \sum \varepsilon_i \sin^2 \theta_i$, where ε_i is the kinetic energy of each fragment and θ_i is the angle between the fragment and the beam direction. We choose the transversal energy as our observable *and* assume that it is proportional to the excitation energy E of the source [26, 27], where $E_t \cong K(E_{beam}, A_P, A_T)E$.

From Eqs. 5 and 6, we extract the elementary probability p and m from the mean and variance of the experimental multiplicity distributions for the ^{36}Ar + ^{197}Au reactions at E/A=80 and 110 MeV. At this point we need to consider the effect of the device efficiency ε on the fold probabilities, the mean multiplicity and its variance, and finally, on the observed probability p_{obs}. Disregarding details associated with anisotropies, multiple hits, etc, we can estimate that the true probability p is simply related to the observed probability p_{obs} by the relationship $p_{obs} = \varepsilon p$. This observed probability p_{obs} should combine exactly like p in the binomial expressions (Eqs. 4 - 7). The geometric efficiency of the Miniball is 0.89 [22] and represents an upper limit for the device

efficiency in the experiment quoted above. The derived values of p_{obs} should be corrected by the device efficiency ε to obtain the physical probability p.

In Fig. 1 we plot m as a function of E_t for the intermediate mass fragments multiplicity distributions (circles) and for the total charged particle multiplicity distributions (diamonds). In Fig. 2a, we plot $\log 1/p$ vs. $E_t^{-1/2}$ for the fragment distributions (Arrhenius plot). If the probability p is thermal, as given in Eq. 2, this plot ought to be linear[19] since $T \propto \sqrt{E}$. The linearity of this plot over two orders of magnitude is stunning, and strongly suggests the "thermal" nature of p. The straight lines obtained for the two bombarding energies suggest that the simple proportionality law between E_t and E is satisfied. The difference in slopes suggests that the proportionality constant is bombarding energy dependent.

One can also extract p "differentially" (Eq. 7) by considering the ratios P_n / P_{n+1} from the experimental excitation functions. For each bombarding energy, all of the experimental excitation functions ($n \leqq 4$) tightly collapse onto a straight line as shown in Fig. 2b, when subjected to the above procedure.

We also show a comparison (see Fig. 3) between the experimental excitation functions and those calculated using the values of p obtained from the linear fits of Fig. 2 and the associated values of m from Eq. 5. The extraordinary quantitative agreement between the calculations and the experimental data confirms the binomiality of the multifragmentation process.

^{129}Xe-Induced Reactions

To compare with the results of the ^{36}Ar + ^{197}Au reactions, we have studied the reactions of ^{129}Xe + ^{197}Au at three bombarding energies. In this analysis, 0.1% of the total number of events at the tail of the E_t distribution (large E_t) is excluded due to the lack of statistics. The corresponding values of P_n are plotted in Fig. 4b for n =0 to n=9, together with the solid lines generated from the binomial distribution in Eq. 4. The input values for p and m in Eq. 4 are extracted from the mean $< n >$ and the variance σ^2 of the fragment multiplicity by using Eqs. 5 and 6. An excellent agreement between the experimental n-fold fragment emission probabilities (symbols) and the binomial calculations (curves) for the entire E_t range is observed for values of n

up to 9 at all three bombarding energies. This remarkable agreement means that the probability P_n is indeed binomial and can be reduced to an elementary probability p for one fragment emission.

To investigate the temperature dependence of the elementary probability p, the natural logarithm of $(1/p)$ or correspondingly the ratio τ/τ_o is plotted as a function of $E_t^{-1/2}$ in Fig. 4a for the ^{129}Xe + ^{197}Au reactions. A linear dependence is observed for all three bombarding energies similar to the pattern observed for ^{36}Ar + ^{197}Au reactions at E/A = 80 & 110 MeV. The solid lines are linear fits to the data. The linearity of these plots is additional evidence for the "thermal" nature of p over the excitation energy range measured.

The values of p obtained "differentially" using Eq. 7 can be compared with those calculated "integrally" using Eqs. 5 and 6. Fig. 5 shows the differentially determined values of p up to n=4 collapse onto the straight lines taken from Fig. 4a for all three bombarding energies. The good consistency between the two different methods of extracting p confirms the binomial nature of P_n and the thermal dependence of p.

At this point we proceed to consider the reactions using lighter targets. The experimental n-fold fragment emission probabilities for these reactions are obtained following the same procedure used for the ^{129}Xe + ^{197}Au analysis. Fig. 6 shows the excitation functions for ^{129}Xe-induced reactions on ^{nat}Cu, ^{89}Y, and ^{165}Ho targets at E/A = 40MeV. As the mass of the target increases, the available energy in the center of mass frame increases from 1710 MeV to 2895 MeV, and hence the excitation energy increases accordingly. The observed increase in the range of the transversal energy with increasing target mass in Fig. 6 is consistent with our assumption that the transversal energy is proportional to excitation energy.

Interestingly, the excitation functions are similar for all three targets over the entire range of the transversal energy. This prompts one to compare their extracted values of p and m. A most remarkable result is that the Arrhenius plots for different targets collapse onto a nearly universal line, and the binomial parameter m is also independent of the target mass as shown in Fig. 7 for the ^{129}Xe-induced reactions at E/A = 40 MeV. For the ^{nat}Cu and ^{89}Y, where the target masses

are lighter than ^{129}Xe, this near target independence suggests that the multifragmentation source is the incomplete fusion product formed when the ^{129}Xe projectile picks up various amounts of mass from any target. In other words, the source can be characterized mainly by the amount of mass transfer, and the reactions depend relatively little on the actual nature of the target[28]. For the heavier ^{165}Ho and ^{197}Au targets, the incomplete fusion model predicts dominant formation of target-like sources by picking up mass from the lighter ^{129}Xe projectile. The structure of these target-like sources should be different from that of the projectile-like sources. However, the same target independence is observed for the heavier ^{165}Ho and ^{197}Au targets as shown in Fig. 7. One immediate implication seems to be that for ^{129}Xe-induced reactions, there is always a dominant projectile-like source independent of the target mass[28]. This picture is certainly not conventional within the incomplete fusion model, and remains an unresolved puzzle. The extracted values of p and m are used to generate the curves shown in Fig. 6. The excellent agreement between the data and binomial calculations confirms the binomial nature of P_n and its reducibility to p independent of the specific target. In addition, ^{129}Xe-induced reactions at the two higher bombarding energies (E/A = 50 and 60 MeV) studied also shows a similar target independence.

Discussion

The more directly interpretable physical parameter contained in this analysis is the binary barrier B (proportional to the slope of the data in Fig. 2). One may wonder why a single binary barrier suffices, since mass asymmetries with many different barriers may be present. This is an old problem. Let us consider a barrier distribution as a function of mass asymmetry x of the form $B = B_o + ax^n$, where B_o is the lowest barrier in the range considered. Then,

$$p = \frac{\Gamma}{\hbar\omega_o} = \int e^{-B_o/T} e^{-ax^n/T} dx \cong \left(\frac{T}{a}\right)^{1/n} e^{-B_o/T} . \qquad (8)$$

Thus the simple form of Eq. (2) is retained with a small and renormalizable pre-exponential modification.

One possible interpretation of the reducibility discussed above is sequential decay with constant probability p. Assuming that the (small) fragments, once produced do not generate additional fragments or disappear, the binomial distribution follows directly. In this framework, it is possible to translate the probability p into the mean time separation between fragments. In other words, we can relate the n-fragment emission probabilities to the mean time separations between fragments. The validity of this interpretation is testable by experiment.

Equation 3 shows that the decay probability and the associated decay lifetime are dramatically affected even by moderate changes in temperature. Furthermore, as the temperature becomes comparable with the barrier, the binary decay probability approaches unity and the lifetime approaches the characteristic (dynamical) time constant of the channel, τ_o. This behavior is indeed shown by the extracted times ($\tau = \tau_o/p$) shown in Fig. 2.

To measure the mean time separation between fragments, groups have utilized the pairwise fragment-fragment correlations introduced by their mutual Coulomb interaction. Results have been presented showing a substantial dip in the probability of finding pairs of fragments at small relative velocities[11-15] and small relative angles[10, 16]. Simulations, performed with chemical equilibrium and sequential decay codes, were compared with experiment, and rather short upper limits ($\tau < 100$ fm/c) were obtained for the decay time-scales for central collisions (large values of E_t).

A recent experiment[16] has studied the "proximity" effect of the surviving partner, produced in a deep inelastic-like collision, on the angular distribution of the fragments resulting from the break-up of the other partner. This remarkable experiment shows that at small excitation energies the "proximity" effects are essentially absent, but become very pronounced at large excitation energies. This onset of proximity effects was taken to signify a transition from slow sequential multifragmentation to fast, nearly simultaneous multifragmentation. However, the observed decrease of the decay lifetime with increasing excitation energy [12, 13, 15, 16] is also consistent with what is expected for the energy dependence of sequential decay, and, by itself does not prove a change in mechanism.

The detailed accuracy and the broad applicability of the binomial distribution are somewhat disconcerting. For instance, what is the significance of the parameter m? In the sequential description the system is given m chances to emit a fragment, with fixed probability p, after which the emission is shut off. One might have guessed that the probability p would decrease progressively as a function of time due to evaporative cooling, and that m is just an approximate cut-off made necessary by the constant p in the binomial distribution. This hypothesis, however, may not be correct. A simple evaporation calculation shows that during the time $t = m\tau_0$ ($\hbar\omega_o \cong 1$ MeV) the system has insufficient time to cool completely. Therefore p may be *nearly* constant, and one is led to attribute a more physical significance to m. What switches the emission off after m tries must remain here a speculation. Let us venture to say that dynamics may be responsible for such an effect. Could it be that the fragments are statistically emitted while the system undergoes an expansion phase [29-32] only to be shut off as it reverts to normal density? If it were to be so, this would be a significant dynamical feature in an otherwise rather thermal picture.

To see if the light charged particles give any evidence for a longer cooling time, we performed the same analysis on the total charged particles emitted in these reactions. From the means and variances, one obtains values of m almost four times larger than those obtained for the fragments (see Fig. 1). In our picture, this could be a reflection of a longer total emission time and/or a shorter intrinsic period τ_o for light charged particle emission.

We have tried to find alternative explanations to the sequential description for the binomial distributions with thermal probabilities. An obvious model is a chain of m links with probability p that any of the links is broken. The probability that n links are broken is given by Eq. 4. This result is, of course, strictly dependent on the dimensionality of the model, and its relevance to multifragmentation is unclear. Nevertheless, it stresses again the *fundamental reducibility* of the multifragmentation probability to a binary breakup probability p.

The final proof for or against sequentiality must rest on independent time measurements. The establishment of an agreement between the times inferred from the emission probabilities and from the particle-particle correlations would go a long way toward resolving this issue.

Conclusions

We have studied the production of intermediate-mass-fragments in ^{36}Ar and ^{129}Xe-induced reactions at intermediate energies. The fragment multiplicity distributions as a function of the transversal energy are well described by a binomial distribution characterized by a single binary event probability p. The thermal nature of p is demonstrated by its characteristic energy dependence as shown in Arrhenius plots. These results are strong evidence for the reducibility of P_n to p in intermediate energy heavy-ion reactions. The immediate implications are that all the physics contained in a multifragmentation event can be reduced to the physics of a single fragment emission. In other words, one can derive the probability of emitting n fragments solely from the probability of emitting one. Thus multifragmentation is empirically reducible to single fragment emission.

Under the assumption of sequentiality, the inferred emission time scale contracts rapidly with increasing excitation energy. Such a contraction could explain the observed rapid onset of the fragment-fragment Coulomb interaction with increasing excitation energy and would obviate the need for "simultaneous" multifragmentation as a distinct process. While for very short time scales the distinction between sequential and simultaneous emission may become blurred, the retention of reducibility still conveys a very interesting message regarding the structure of the multifragmentation event.

Acknowledgments

This work was supported by the Director, Office of Energy Research, Office of High Energy and Nuclear Physics, Nuclear Physics Division of the US Department of Energy, under contract DE-AC03-76SF00098 and by the National Science Foundation under Grant Nos. PHY-8913815, PHY-90117077, and PHY-9214992

Present addresses:
[a]INFN, Via Amendola 173, 70126 Bari, Italy
[b]Heavy Ion Laboratory, Warsaw University, Poland
[c]Chalk River Laboratories, Chalk River, Ontario, Canada K0J 1J0
[d]Instituto de Fisica, Universidade de Sao Paulo, C.P. 20516, CEP 01498, Sao Paulo, Brazil
[e]Lawrence Berkeley Laboratory, Berkeley CA 94720
[f]National Laboratory for High Energy Physics, 1-1 Oho, Tsukuba, Ibaraki 305, Japan
[g]GANIL BP 5027, F-14021 Caen, France
[h]Physics Department, Hope College, Holland MI
[i]Gesellschaft fur Schwerionenforschung, D-6100 Darmstadt, Germany
[j]Indiana University Cyclotron Facility and Department of Chemistry, Indiana University, Bloomington, IN 47405
[k]Brookhaven National Laboratory, Upton, Long Island, NY 11973

References

[1] L. G. Sobotka, et al., Phys. Rev. Lett. **51**, 2187 (1983).

[2] L. G. Moretto and G. J. Wozniak, Prog. Part. & Nucl. Phys. **21**, 401 (1988).

[3] D. Guerreau, *Formation and Decay of Hot Nuclei: The Experimental Situation* ed. (Plenum Publishing Corp., 1989).

[4] H. H. Gutbrod, A. M. Poskanzer, and H. G. Ritter, Rep. Prog. Phys. **52**, 1267 (1989).

[5] D. H. E. Gross, Rep. Prog. Phys. **53**, 605 (1990).

[6] L. G. Moretto and G. J. Wozniak, Ann. Rev. Part. & Nucl. Sci **43**, 379 (1993).

[7] J. Aichelin, Phys. Rep. **202**, 233 (1991).

[8] B. Borderie, Ann. Phys. Fr. **17**, 349 (1992).

[9] O. Schapiro and D. H. E. Gross, Nucl. Phys. A **573**, 143 (1994).

[10] T. Ethvignot, et al., Phys. Rev. C **48**, 618 (1993).

[11] D. Fox, et al., Phys. Rev. C **47**, R421 (1993).

[12] E. Bauge, et al., Phys. Rev. Lett. **70**, 3705 (1993).

[13] D. R. Bowman, et al., Phys. Rev. Lett. **70**, 3534 (1993).

[14] T. C. Sangster, et al., Phys. Rev. C **47**, R2457 (1993).

[15] M. Louvel and et. al., Phys. Lett. B **320**, 221 (1994).

[16] M. Aboufirassi, et al., LPC Caen preprint LPCC 94-02 (1994).

[17] A. Lleres, et al., ISN Grenoble ISN 94-33 (1994).

[18] T. Glasmacher, et al., Phys. Rev. C **50**, 952 (1994).

[19] L. G. Moretto, D. N. Delis, and G. J. Wozniak, Phys. Rev. Lett. **71**, 3935 (1993).

[20] J. Pouliot, et al., Phys. Rev. C **48**, 2514 (1993).

[21] In chemical reactions the rate, r often obeys the relation $r = r_0 \exp[-B/T]$, where B is the activation energy. The plot of log$r$ vs $1/T$ is therefore linear and is called an Arrhenius plot. In the nuclear case $T \propto E^{1/2}$, thus one plots log$r$ vs $1/E^{1/2}$.

[22] R. T. de Souza, et al., Nucl. Instr. and Meth. A **295**, 109 (1990).
[23] W. L. Kehoe, et al., Nucl. Instr. Meth. Phys. Res. **A311**, 258-72 (1992).
[24] L. Phair, et al., Phys. Lett. B **291**, 7 (1992).
[25] L. Phair, Ph.D. thesis, Michigan State University, 1993.
[26] R. Bougault , et al., LPC Caen LPCC 94-04 (1994).
[27] In a geometric model, the intrinsic excitation is a function of the impact parameter. Here we neglect any dependence of K on impact parameter.
[28] D. R. Bowman, et al., Phys. Rev. **C46**, 1834 (1992).
[29] W. A. Friedman, Phys. Rev. C **42**, 667 (1990).
[30] R. T. de Souza, et al., Phys. Lett. B **300**, 29 (1993).
[31] S. C. Jeong and et al., Phys. Rev. Lett. **72**, 3468 (1994).
[32] W. C. Hsi, Phys. Rev. Lett., in press (1994).

Figure Captions

Fig. 1 The extracted values of $m = \langle n \rangle^2 / \left(\langle n \rangle - \sigma_n^2 \right)$ as a function of the transverse energy E_t for the reaction $^{36}Ar + ^{197}Au$ at E/A = 80 (open symbols) and 110 MeV (solid symbols). The circles correspond to m values extracted from the intermediate mass fragment distributions ($3 \le Z \le 20$) while the diamonds correspond to m values extracted from the total charged particle distributions.

Fig. 2 For the reaction $^{36}Ar + ^{197}Au$ at E/A = 80 (open symbols) and 110 MeV (solid symbols), a) the reciprocal of the binary decay probability $1/p$ or the ratio τ / τ_o (calculated from the mean and variance of the intermediate mass fragment distributions) as a function of $E_t^{-1/2}$. The solid lines are linear fits to $\log(1/p)$. b) Values of $1/p$ extracted "differentially" using Eq. 7 in the text. The solid lines are fits to the data shown in the upper panel and the different symbols represent the ratios extracted with different values of n.

Fig. 3 A comparison between the experimental probability (symbols) and the calculated probability (solid lines) to emit n intermediate mass fragments ($3 \le Z \le 20$) as a function of E_t for the reaction $^{36}Ar + ^{197}Au$ at E/A = 80 (lower panel) and 110 MeV (upper panel). For numbers of fragments n = 0-8, $P(n)$ is calculated assuming a binomial distribution (see Eq. 4) with the values of p obtained from the linear fits shown in Fig. 2 and the corresponding values of m from Eq. 5.

Fig. 4 For the $^{129}Xe + ^{197}Au$ reactions are shown: a) (left column) the reciprocal of the binary decay probability $1/p$ as a function of $E_t^{-1/2}$; and b) (right column) the parameter m and the n-fold intermediate mass fragment ($3 \le Z \le 20$) emission probability $P(n)$ as a function of the transversal energy E_t. The three rows correspond to different bombarding energies: E/A = 40 MeV (upper); E/A = 50 MeV (middle); and E/A = 60 MeV (lower).

Fig. 5 For the reaction $^{129}Xe + ^{197}Au$, the probability p extracted "differentially" using Eq. 7 in the text is shown as a function of $E_t^{-1/2}$. The solid lines are linear fits to $\log(1/p)$, which is calculated from the mean and variance of the intermediate mass fragment distributions.

The different symbols represent the probabilities p extracted "differentially" with different values of n. The three rows correspond to different bombarding energies: E/A = 40 MeV (upper); E/A = 50 MeV (middle); and E/A = 60 MeV (lower).

Fig. 6 A comparison between the experimental (symbols), and the calculated probabilities (solid lines) to emit n intermediate mass fragments ($3 \leq Z \leq 20$) as a function of E_t for E/A = 40 MeV ^{129}Xe induced reactions on different targets: ^{nat}Cu (lower panel), ^{89}Y (middle panel) and ^{165}Ho (upper panel). For number of fragments n = 0-10, $P(n)$ is calculated assuming a binomial distribution with the values of m and p shown in Fig. 7.

Fig. 7 The binomial parameter m (top panel) and the reciprocal of the binary decay probability $1/p$ (bottom panel) as a function of $E_t^{-1/2}$ for ^{129}Xe induced reactions with different targets (^{nat}Cu, ^{89}Y, ^{165}Ho, ^{197}Au) at E/A = 40MeV.

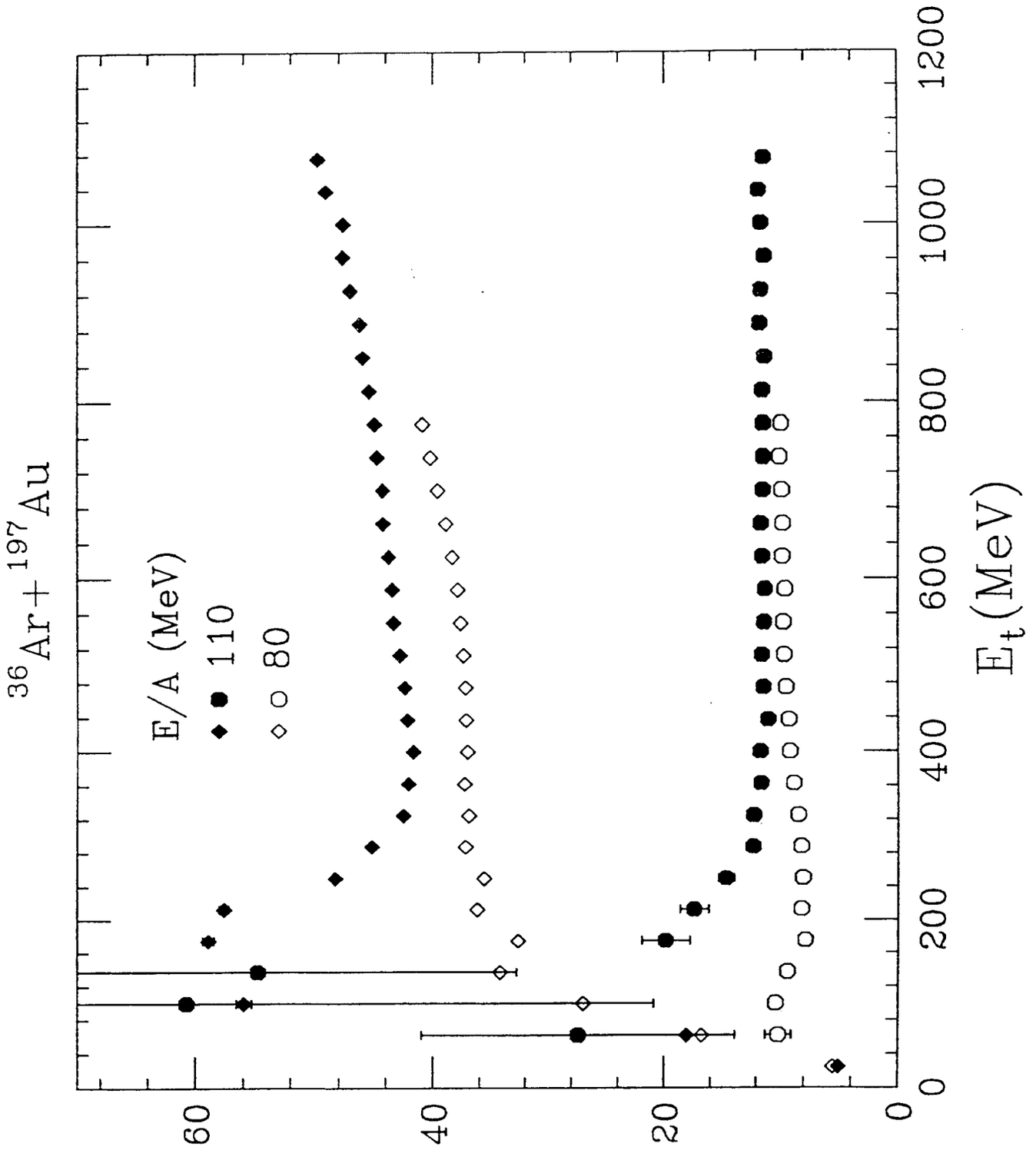
$^{36}Ar + ^{197}Au$
E/A (MeV)
110
80
E_t (MeV)
0
200
400
600
800
1000
1200
0
20
40
60

Fig. 1

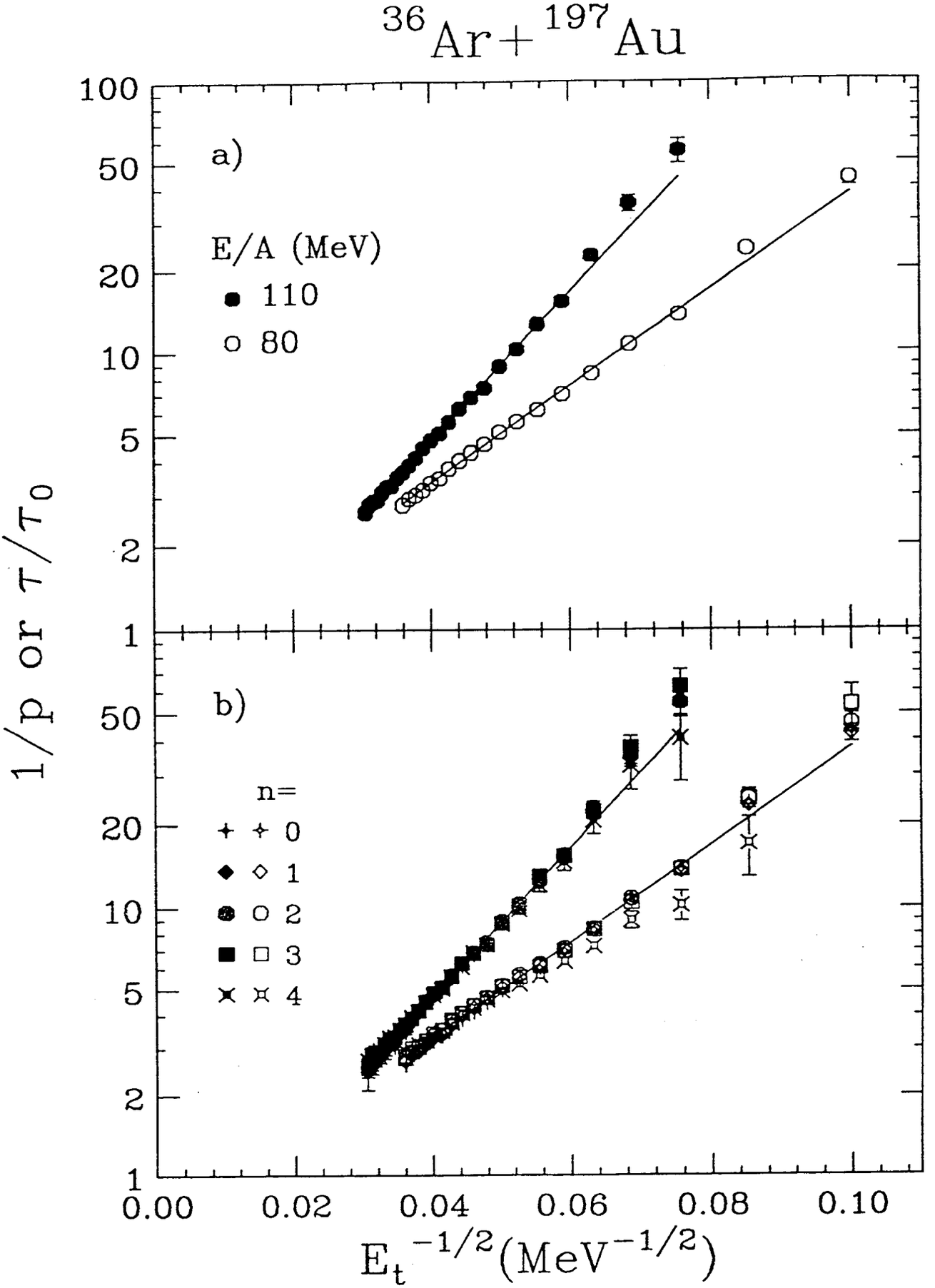
$^{36}Ar + ^{197}Au$
a)
E/A (MeV)
110
80
b)
n=
0
1
2
3
4
$1/p$ or τ/τ_0
$E_t^{-1/2}(MeV^{-1/2})$
100
50
20
10
5
2
1
0.00
0.02
0.04
0.06
0.08
0.10

Fig. 2

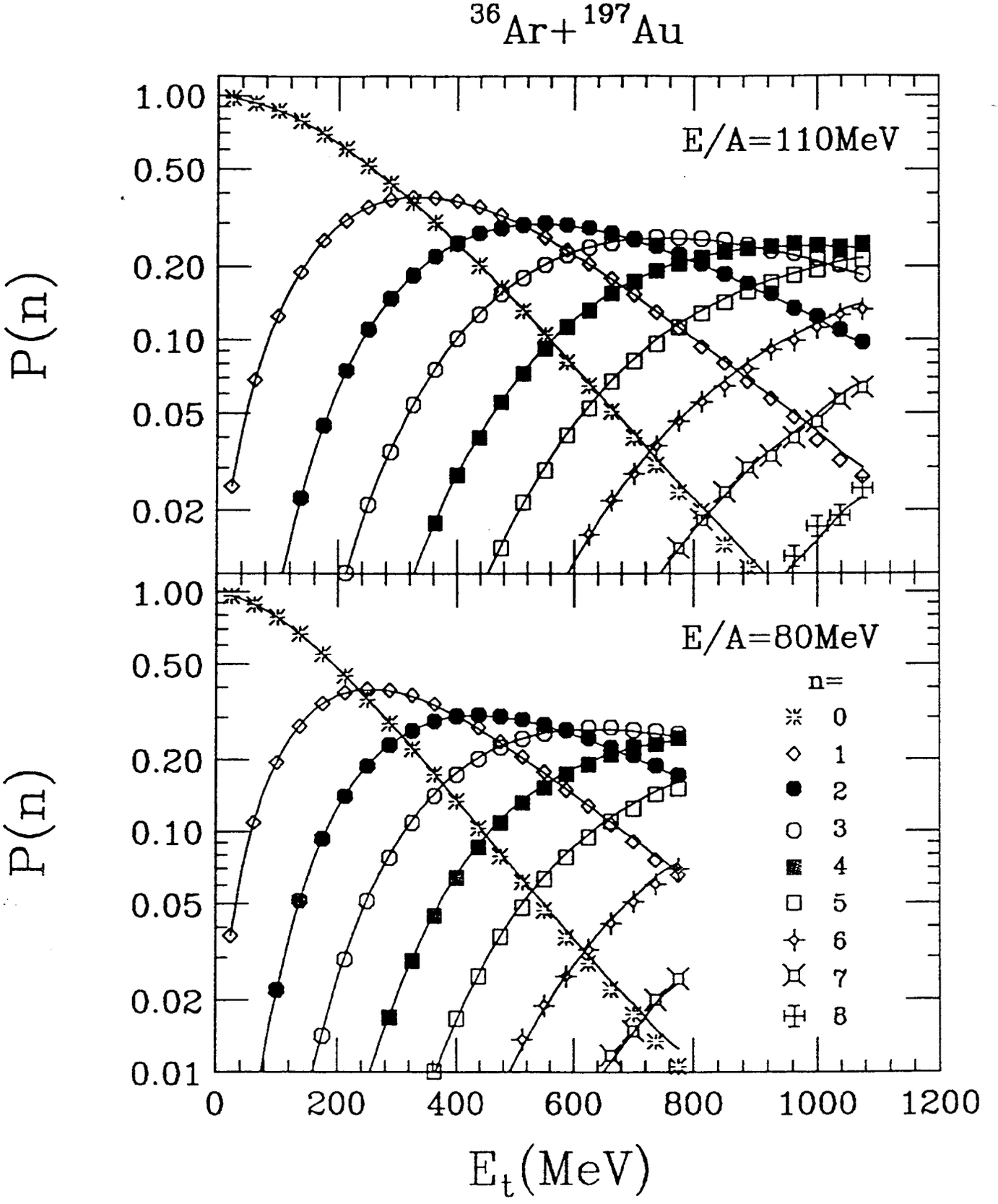
$^{36}Ar+^{197}Au$
E/A=110MeV
E/A=80MeV
P(n)
P(n)
1.00
0.50
0.20
0.10
0.05
0.02
0.01
n=
0
1
2
3
4
5
6
7
8
0
200
400
600
800
1000
1200
E_t(MeV)

Fig. 3

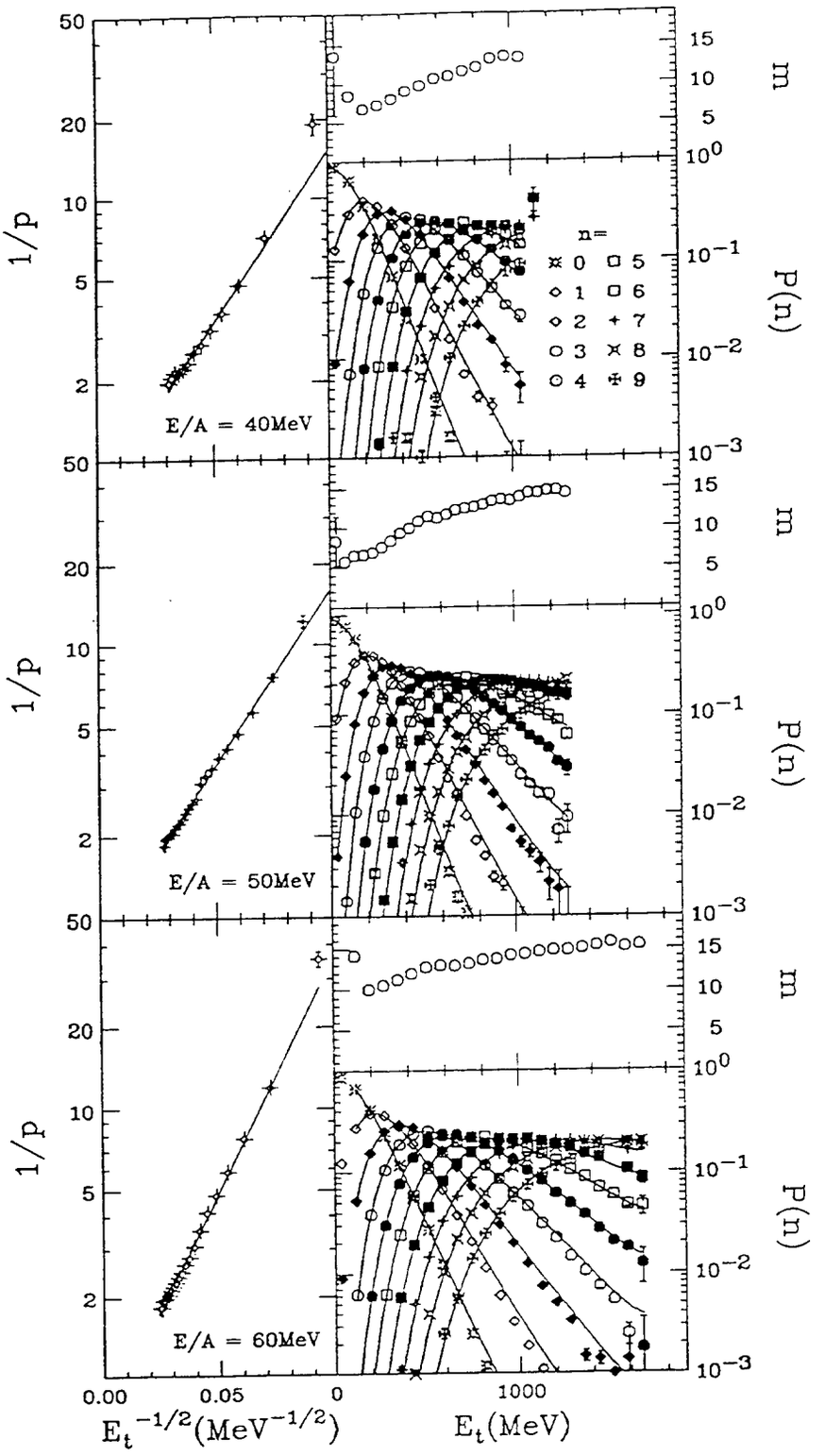
$^{129}Xe+^{197}Au$
1/p
m
P(n)
n=
0 1 2 3 4 5 6 7 8 9
E/A = 40MeV
E/A = 50MeV
E/A = 60MeV
$E_t^{-1/2}(MeV^{-1/2})$
$E_t(MeV)$

Fig. 4

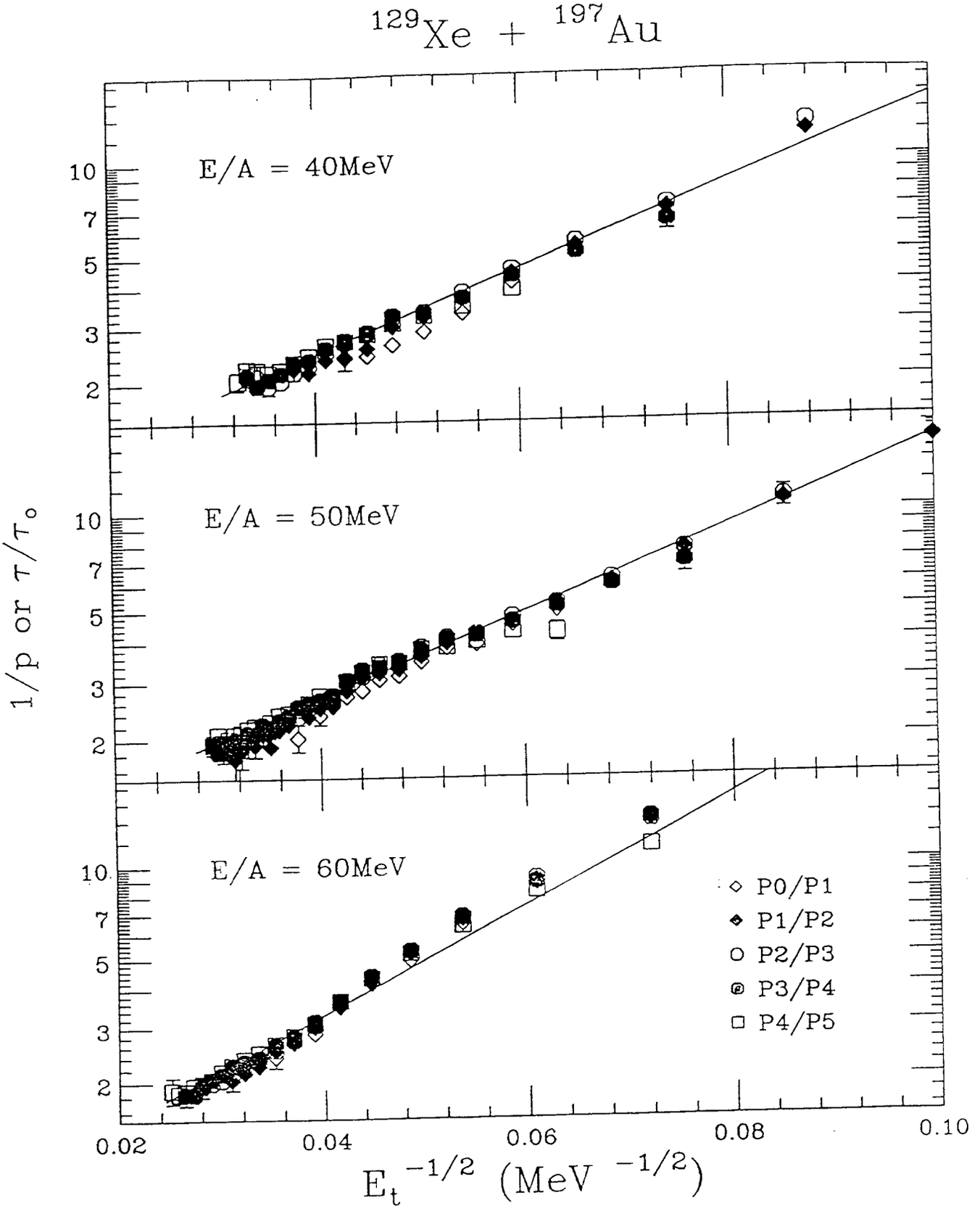
$^{129}Xe + ^{197}Au$
E/A = 40MeV
E/A = 50MeV
E/A = 60MeV
P0/P1
P1/P2
P2/P3
P3/P4
P4/P5
1/p or τ/τ₀
$E_t^{-1/2}$ (MeV $^{-1/2}$)
10
7
5
3
2
0.02
0.04
0.06
0.08
0.10

Fig. 5

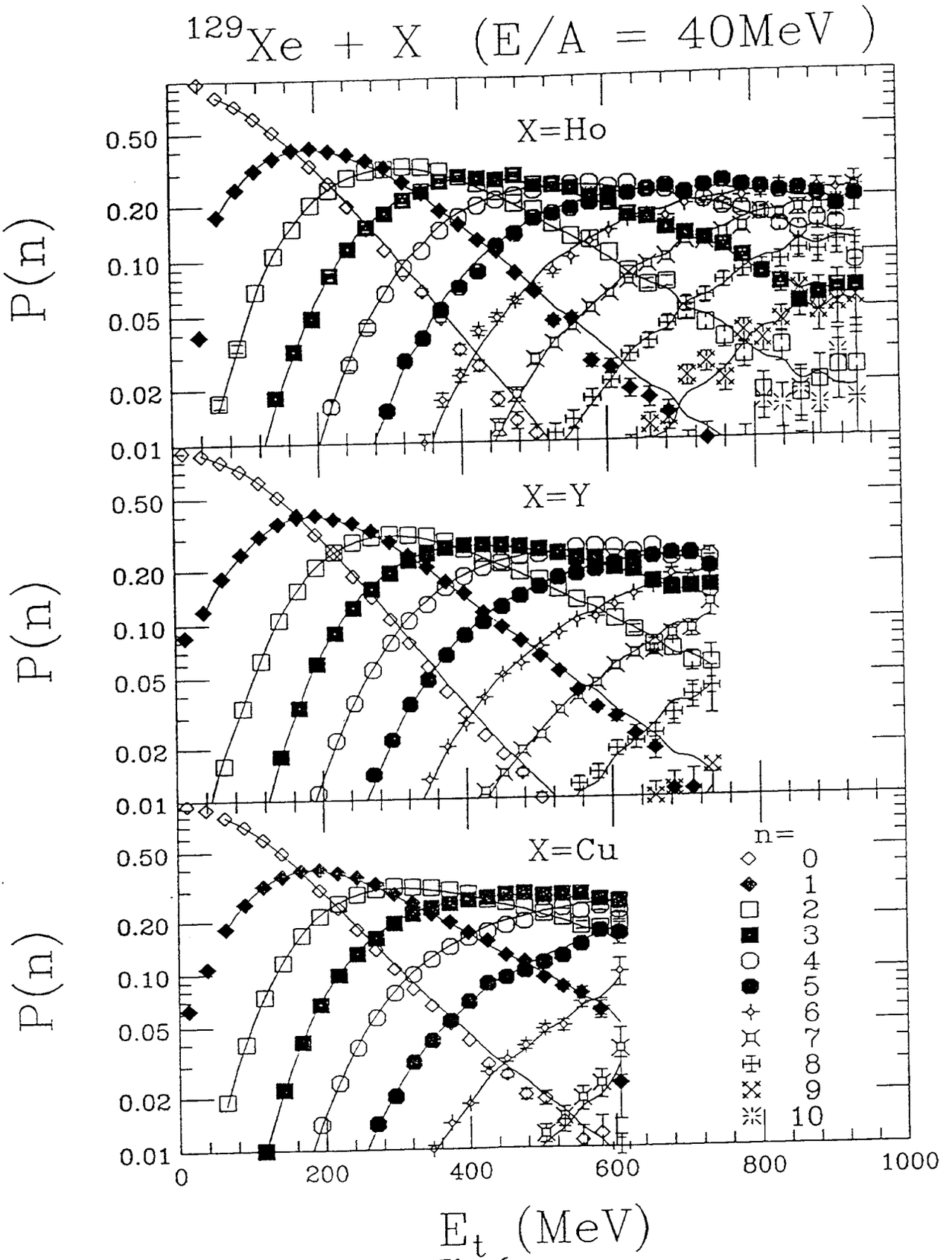
^{129}Xe + X (E/A = 40MeV)
X=Ho
X=Y
X=Cu
P(n)
P(n)
P(n)
0.50
0.20
0.10
0.05
0.02
0.01
n=
0
1
2
3
4
5
6
7
8
9
10
0
200
400
600
800
1000
E_t (MeV)

Fig. 6

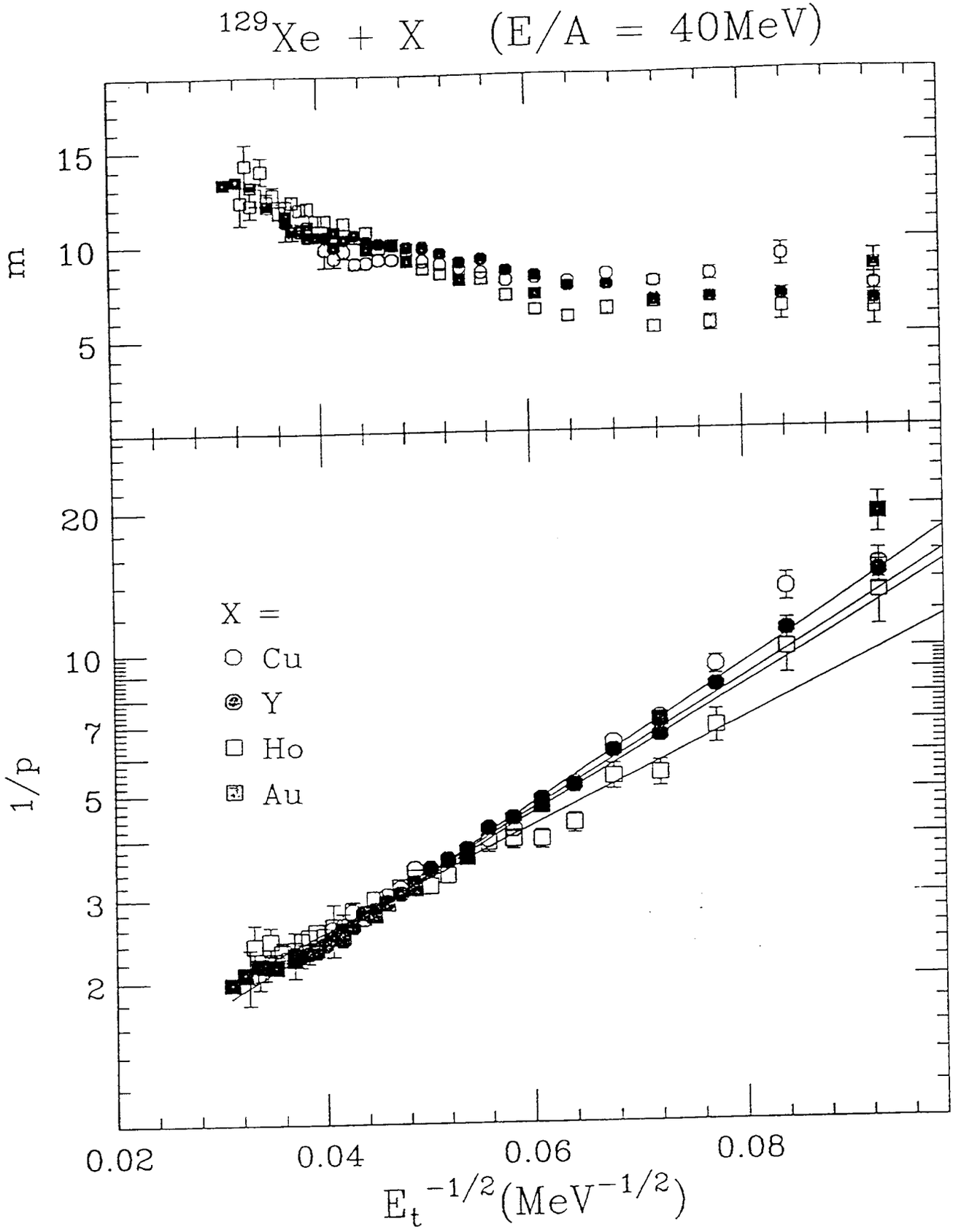
^{129}Xe + X (E/A = 40MeV)
m
15
10
5
1/p
20
10
7
5
3
2
X =
Cu
Y
Ho
Au
0.02
0.04
0.06
0.08
$E_t^{-1/2}(MeV^{-1/2})$

Fig. 7